

NATIONAL ADVISORY COMMITTEE FOR AERONAUTICS

TECHNICAL NOTE 3977

FURTHER EXPERIMENTS ON THE STABILITY OF LAMINAR AND
TURBULENT HYDROGEN-AIR FLAMES
AT REDUCED PRESSURES

By Burton Fine

Lewis Flight Propulsion Laboratory
Cleveland, Ohio

LIBRARY COPY

APR 11 1957

LANGLEY AERONAUTICAL LABORATORY
LIBRARY, NACA
LANGLEY FIELD, VIRGINIA



FOR REFERENCE

Washington

April 1957

NOT TO BE TAKEN FROM THIS ROOM



3 1176 01425 9098

NATIONAL ADVISORY COMMITTEE FOR AERONAUTICS

TECHNICAL NOTE 3977

FURTHER EXPERIMENTS ON THE STABILITY OF LAMINAR AND
TURBULENT HYDROGEN-AIR FLAMES AT REDUCED PRESSURES

By Burton Fine

SUMMARY

Stability limits for laminar and turbulent hydrogen-air burner flames were measured as a function of pressure, burner diameter, and composition. The average pressure exponent of the critical boundary velocity gradient for turbulent flashback was 1.31, which is not significantly different from the laminar value. The use of a simple flame model and measured turbulent flame speeds indicated that turbulent flashback could involve a smaller effective penetration distance than laminar flashback. Turbulent blowoff velocity was nearly independent of pressure and varied about as the inverse square root of the burner diameter. Of several recent theoretical treatments, none satisfactorily predicts the observed dependence of blowoff on pressure and burner diameter. Extrapolation of stability loops to the quenching point showed that the quenching pressure was inversely proportional to burner diameter. The actual pressures were higher than those obtained by other quenching measurements.

INTRODUCTION

Relatively little attention has been paid to the stability limits of turbulent burner flames as a function of pressure. Reference 1 (p. 82) reports data on the flashback of unpiloted turbulent propane-air flames at pressures above 1 atmosphere. It was observed that the critical boundary velocity gradient was several times higher than that for corresponding laminar flames at the same pressure and composition. Reference 2 presents blowoff and flashback data for acetylene flames at low pressures; these data extend into the turbulent region. However, data in the higher Reynolds number region are not discussed in detail.

The present study is concerned with the stability of unpiloted turbulent hydrogen-air flames at subatmospheric pressures and extends, into the turbulent region, previous work done on properties of laminar

4200

CQ-1

hydrogen-air flames at subatmospheric pressures (ref. 3). Turbulent flashback was studied at various pressures, equivalence ratios, and burner diameters. Results are compared with results in the laminar region. A possible explanation of the results based on the extension of the laminar model to the case of turbulence is offered. Blowoff in the turbulent region was studied at various pressures and burner diameters at equivalence ratios of 1.1 and 1.5. The results are compared with predictions of several recent theoretical treatments, none of which give satisfactory predictions.

Several stability loops were obtained. These permitted an estimation of the dependence of quenching distance on pressure. The results were in reasonable agreement with those obtained by more direct measurements of flame quenching (ref. 4).

SYMBOLS

A,C	dimensionless coefficients
D	burner diameter, cm
g	critical boundary velocity gradient, sec^{-1}
k	pressure exponent, dimensionless
l	thickness of laminar sublayer, cm
M	molar weight, g
m	diameter exponent, dimensionless
n	pressure exponent of burning velocity, dimensionless
P	ambient pressure, cm Hg
q	quenching point, dimensionless
R	gas constant, $\text{cal}/(\text{mole})(^\circ\text{K})$
r	radial distance, cm
Re	Reynolds number, dimensionless
S	flame surface, sq cm
T	temperature, $^\circ\text{K}$
U	velocity, cm/sec
\bar{U}	mean stream velocity, cm/sec

V volume flow, cm^3/sec
 β' stability parameter, dimensionless
 δ penetration distance, cm
 μ viscosity, poises
 ν kinematic viscosity, cm^2/sec
 ϕ equivalence ratio, fuel-air ratio divided by fuel-air ratio for stoichiometric mixture

Subscripts:

av average
b burning
bo blowoff
cr critical for laminar-turbulent transition
f flashback
p constant pressure
q quenching
t turbulent
w wall

Superscript:

o determined at calibration conditions (near 1 atm) or initial conditions

APPARATUS AND PROCEDURE

The apparatus used was that described in reference 3. It is shown schematically in figure 1. Burner flames were established within a chamber whose pressure was regulated by a vacuum pump and manual air bleed. The pressure within the chamber was read on a manometer. The burner itself was 50 inches long and about $3/4$ inch in diameter and was water cooled near the lip. Tubular inserts of about $4/10$ and $5/8$ inch were used. Tank hydrogen (98 to 99 percent hydrogen) and tank compressed

air (water-pumped) were used without further purification. The combustible mixture was prepared by metering fuel and air separately through calibrated critical-flow orifices and mixing several feet upstream of the burner inlet.

For measuring stability limits a stable flame was established at some pressure. Then the pressure was slowly increased or decreased at constant mass flow until the flame flashed back or blew off. The average stream velocity at which flame loss occurred was obtained as a function of ambient pressure, burner diameter, and nominal volume flow rate at the calibration pressure (about 1 atm) by the expression

$$\bar{U}_f \text{ (or } \bar{U}_{bo}) = \frac{4V^0}{\pi D^2} \frac{P^0}{P} \quad (1)$$

This procedure is essentially that described in reference 2. Near the quenching point flames did not flash back sharply, but rather moved slowly back into the tube. Often this movement was asymmetric and resulted in tilted flames (ref. 5). In this region, the flashback pressure was taken as the pressure at which a portion of the flame first dropped below the level of the burner rim.

Turbulent flame speeds were measured by the method of reference 6. Flames were photographed, and the mean flame surface was obtained from measurement of the visible image. With simple photographic means, measurable images were obtained down to pressures of about 0.3 atmosphere. The flame speeds were then obtained by the relation

$$U_{b,t} = \frac{V^0}{S_m} \frac{P^0}{P} \quad (2)$$

No correction was made for the effect of flame-front curvature on the apparent mean flame surface. All measurements were made on a 4/10-inch (1.016-cm) burner at a Reynolds number of about 3500.

RESULTS AND DISCUSSION

Flashback

The flashback of a laminar burner flame is generally described by a critical boundary velocity gradient. This gradient is related to other flame properties by the expression

$$g_f = U_b/\delta \quad (3)$$

where δ is the penetration distance, the smallest distance from a cold wall at which the burning velocity attains its normal value (ref. 7, p. 285). If it is assumed that some similar model applies to the flashback of turbulent flames, equation (3) may be written as

$$g_{f,t} = (U_b/\delta)_t \quad (4)$$

where turbulence may affect U_b and δ .

Calculation of velocity gradients. - For a flame on a cylindrical burner with fully developed laminar pipe flow, the expression

$$g_f = \left(\frac{dU}{dr} \right)_w = \frac{8\bar{U}_f}{D} \quad (5)$$

is a good approximation provided it is assumed that δ/D is small. This is equivalent to the assumption that the burner diameter is much larger than the quenching diameter at a given pressure.

For turbulent pipe flow, the expression for the boundary velocity gradient (based on the existence of a laminar sublayer near the wall) given by reference 7 (p. 285) is

$$g_t = 0.023 \text{ Re}^{0.8} \frac{\bar{U}}{D} \quad (6)$$

where Reynolds number is defined as

$$\text{Re} = \frac{\bar{U}D}{\nu} \quad (7)$$

At flashback equation (6) takes the form, in terms of convenient laboratory variables,

$$g_{f,t} = 0.023 \left(\frac{\mu RT}{M} \right)^{-0.8} p^{0.8} \bar{U}^{1.8} D^{-0.2} \quad (8)$$

For the present study the gases were assumed ideal; thus the molecular weight was additive in the mole fraction. The mixture viscosity μ was obtained by an approximation given in reference 8. It was found that, within experimental accuracy, the viscosity for mixtures containing between 25 and 50 percent hydrogen by volume could be assumed constant and equal to 0.000179 poise. The same value of μ was used for the few data points obtained outside the composition range given above, at 17 and 56 percent hydrogen. The error is not significant.

Experimental results for flashback are shown in figure 2 and tables I and II. Values of laminar and turbulent critical boundary velocity gradients were calculated by equations (5) and (6), respectively. Most of the data in the laminar region are from reference 3. However, points in the quenching region for $D = 1.016$ centimeters, $\phi = 1.1$ and 1.5 for $D = 1.459$ centimeters, $\phi = 1.1$ are new. Some of the new data are used in both figures 2 and 5, the rest in figure 5 only.

The derivation of the expression for $g_{f,t}$ involves an empirical friction factor which applies only in the region of fully developed turbulence and not in the region of laminar-turbulent transition. Experimental data on pipe friction (e.g., ref. 9, p. 402) indicate that the transition region lies between Reynolds numbers of 2200 and 3200. However, flashback data of figure 2 indicate that the transition region, taken to be that region where the ambient pressure at flashback is independent of the critical stream velocity for a given burner, lies between Reynolds numbers of 1500 and 2500. That is, the transition region is displaced by a Reynolds number of 700. Below $Re = 1500$, equation (5) correlates the data. Above $Re = 2500$, equation (6) gives a good correlation. Because of the displacement of the transition region, no attempt was made to obtain a friction factor for that region from pipe friction data. Instead, flashback velocity gradients were calculated by the laminar expression (eq. (5)) up to the point where the flames appeared visibly and steadily turbulent and the pressure at flashback was no longer independent of Reynolds number. Since the pressure remained constant in the transition region, a more sophisticated calculation would not have altered the curve in any way but would merely have shifted data points along the curves to slightly higher values of g_f . Qualitative measurement of longitudinal velocity fluctuation with a hot-wire anemometer showed that, in the absence of a flame, the flow at the center of the tube mouth (for $D = 1.89$ and 1.459 cm) was laminar below a Reynolds number of about 1500. Between Reynolds numbers of 1500 and 2500 the flow was generally laminar but showed an increasing frequency of turbulent pulsations with increasing Reynolds number. Above $Re = 2500$, the flow was steadily turbulent. Thus the cold-flow behavior correlated well with the flame behavior. This showed that the apparent displacement of the laminar-turbulent transition was characteristic of the tube and was probably not a flame-induced effect.

Effect of pressure and tube diameter. - Figure 2 shows that between equivalence ratios of 0.80 and 2.25 (25 and 48 percent-hydrogen) the pressure exponent of the critical boundary velocity gradient for flashback in the turbulent region $\partial \log g_{f,t} / \partial \log P$ varies in the range 1.22 to 1.44, the variation with composition being random. The average value is 1.31. Since the pressure exponent of the critical boundary velocity gradient for the laminar flames was 1.35 ± 0.08 (ref. 3), the

pressure exponents for the laminar and turbulent case are the same, within experimental error. This is to be expected if the boundary velocity gradient at flashback is proportional to a reaction rate (ref. 10).

Experimental results indicate that the average stream velocity at flashback is correlated by a relation of the form

$$\bar{U}_f = \bar{U}_f^0 P^{k_f} D^{m_f} \quad (9)$$

where \bar{U}_f^0 represents the average flashback velocity at 1 atmosphere for a burner 1 centimeter in diameter. Equation (8) may be combined with equation (9) to give

$$g_{f,t} = 0.023 \bar{U}_f^{0.1.8} \left(\frac{\mu R T}{M} \right)^{-0.8} P^{(0.8+1.8 k_f)} D^{(-0.2+1.8 m_f)} \quad (10)$$

which expresses the pressure and diameter dependence of the critical boundary velocity gradient in terms of the pressure and diameter dependence of the critical mean stream velocity. By equations (9) and (10)

$$\frac{\partial \log g_{f,t}}{\partial \log P} = 0.8 + 1.8 \frac{\partial \log \bar{U}_{f,t}}{\partial \log P} \quad (11)$$

Since the left side of equation (11) equals about 1.31, the pressure exponent of the critical turbulent flashback velocity is about 0.28.

In a similar fashion, the diameter dependence of the critical flashback velocity and boundary velocity gradient are related by the expression

$$\frac{\partial \log g_{f,t}}{\partial \log D} = -0.2 + 1.8 \frac{\partial \log \bar{U}_{f,t}}{\partial \log D} \quad (12)$$

which shows that if the flashback velocity gradient is independent of burner diameter (as seems to be the general case in fig. 2) then the critical mean stream velocity will also be nearly independent and $\partial \log \bar{U}_{f,t} / \partial \log D$ will have a value of about 0.1 at the most.

At an equivalence ratio of 3.00 only a few points could be obtained in the turbulent region. These gave $\partial \log g_{f,t} / \partial \log P = 1.26$, a value in good agreement with the general result. At the lean extreme of the composition range covered, $\phi = 0.50$, a much lower value of $\partial \log g_{f,t} / \partial \log P$ was obtained, about 0.87. Because of the unreliability of the data in this region, no interpretation is put on that result.

Effect of composition. - In reference 3 it is shown that the mean critical laminar flashback velocity and, therefore, the critical laminar boundary velocity gradient, peaked at about $\phi = 1.5$. In the turbulent region, however, the critical velocity peaked at about $\phi = 1.8$, while the boundary velocity gradient peaked, again, near $\phi = 1.5$. The dependence of $g_{f,t}$ on composition at constant pressure is shown in figure 3. Since the viscosity of hydrogen-air mixtures is very nearly constant between $\phi = 0.8$ and 2.4 and enters into equation (8) only to the 0.8 power (ref. 8), it appears that the difference in peak composition shown between the critical mean stream velocity and the critical boundary velocity gradient does not depend on the viscosity but depends on the density, or, in terms of equation (8), on the pressure and molecular weight. The fact that critical flashback gradients for both laminar and turbulent flames peak at the same equivalence ratio is consistent with the concept that the critical boundary velocity gradient for flashback is proportional to a reaction rate.

Comparison of laminar and turbulent flashback. - Since, within experimental error, the pressure exponents for laminar and turbulent flashback are the same over a range of composition, the relation between laminar and turbulent flashback may be expressed as

$$(g_{f,t}/g_f)_p = A \quad (13)$$

where A has a value of about 2.8 and is independent of pressure, burner diameter, and composition. The result represented by equation (13) is similar to that reported in reference 1 (p. 82) for unpiloted turbulent propane-air flames at pressures greater than 1 atmosphere. In reference 3 laminar flashback velocity gradients for hydrogen-air flames are correlated by the relation

$$g_f = 2.6 U_b/D_q \quad (14)$$

Combination of equations (13) and (14) gives, in the turbulent region,

$$g_{f,t} = 7.3 U_b/D_q \quad (15)$$

Equations (13) and (15) may be explained in terms of the penetration of the flame into the laminar sublayer. Measurements of transverse velocity profiles in pipes have shown that the velocity profile in the sublayer is very nearly linear with radial distance. An empirical expression of the thickness of this sublayer is given in reference 9 (p. 407). In terms of the friction factor given in reference 7, it may be expressed as

$$\lambda = 33 \text{Re}^{-0.9} \quad (16)$$

Velocity-profile measurements show that the laminar sublayer does not merge sharply with the fully turbulent region. Rather, there is a large range of δ/D values which correspond to a region of transition between laminar and turbulent friction. It is quite possible that there should exist a range of values of δ greater than that given by equation (16) over which the turbulent contribution would not be significant. Thus, the coefficient 33 in equation (16) is somewhat arbitrary and seems to give a minimum value for the effective thickness of the laminar sublayer. An alternate expression for δ , which is given in reference 11, has the same form as equation (16) but uses a coefficient of 66. Since the velocity profile in the sublayer is linear with radial distance, the boundary velocity gradient may be written as

$$g_t = U_{cr}/\delta \quad (17)$$

If equations (6) and (16) are combined with equation (17), an expression is obtained which relates U_{cr} to the mean flow

$$U_{cr} = 0.75 \bar{U}/Re^{0.1} \quad (18)$$

Thus U_{cr} is nearly proportional to \bar{U} . In the presence of a flame which is about to flash back

$$U_{cr,f} = 0.75 \bar{U}_f/Re^{0.1} \quad (18a)$$

and equation (16) can be combined with equations (14) and (4) to give

$$g_{f,t} = (U_b/\delta)_t = U_{cr,f}/\delta \quad (17a)$$

If the flame penetrates into the laminar sublayer, δ will be less than δ . In that case, U_b must be less than U_{cr} at flashback. For a Reynolds number of 5000, equation (18a) shows that a minimum value of U_{cr} is about $0.3 \bar{U}$. Thus, if the normal burning velocity is less than $0.3 \bar{U}$ at a given pressure, it will be possible for a flame near flashback to penetrate into the laminar sublayer. Since the maximum burning velocity of hydrogen-air flames is about 300 centimeters per second at 1 atmosphere (refs. 3 and 12) and decreases with decreasing pressure, the condition for penetration into the laminar sublayer at flashback will be met as long as the critical average flashback velocity is not much smaller than 1000 centimeters per second.

Table I shows that this condition is generally met. The following is an example based on data of table I:

Reynolds number, Re	5540
Average flashback velocity, \bar{U}_f , cm/sec	1335
Critical velocity, U_{cr} , cm/sec	422
Burning velocity (ref. 3), U_b , cm/sec	270
Ambient pressure, P , cm Hg	52.5

It appears then, that the burning velocity governing flashback is the laminar burning velocity.

Turbulent and laminar burning velocities shown in figure 4 suggest another interesting point. These data show that $U_{b,t}/U_b \leq 1.30$. Thus, regardless of whether flashback is governed by a laminar or turbulent burning velocity, the threefold increase in the critical boundary velocity gradient with turbulence cannot be ascribed to an increase in burning velocity. By equation (4), then, turbulence must lead to a smaller penetration distance. If turbulent flashback is governed by a laminar burning velocity, it follows from equations (4) and (13) that

$$\delta_t = (1/2.8)\delta \quad (19)$$

Thus, the estimate that the quenching distance between parallel plates should be about twice the penetration distance from a single wall holds only for laminar flow. According to present results, this estimate does not apply to pipe turbulence with a laminar sublayer. As long as the increase in flashback velocity gradient cannot be explained by an increase in flame speed, it seems necessary to assume a smaller penetration distance for the turbulent case, even though it is not easy to imagine why this should be so.

Blowoff

Description of results. - Blowoff data are shown in figures 5 to 8. These were obtained at $\phi = 1.1$ and 1.5, values which correspond, respectively, to conditions of maximum flame temperature and maximum chemical reactivity based on flashback (ref. 3). Since both conditions were richer than stoichiometric, it was desirable to examine the effect of the atmosphere near the flame base. Several check points were run with the flame surrounded by a mantle of inert gas. A low annular flow of carbon dioxide was used, which was just sufficient so that the pink tinge which normally surrounds a hydrogen-air flame disappeared near the flame base. In the laminar region no effect on blowoff limits was observed. In the turbulent region blowoff limits were slightly reduced; that is, the blowoff pressure increased slightly for a given mass flow.

This is attributed to the greater sensitivity of turbulent flames to the cooling effect of a secondary jet. The absence of an effect in the laminar region indicated that the dimensions of the combustion chamber were such that the atmosphere near the flame base was inert and that blowoff was not affected by diffusion of secondary air into the flame base.

In figure 5 are shown stability loops for burners 1.016 and 1.459 centimeters in diameter. These include flashback data previously discussed. Figure 6 shows blowoff curves, incomplete in the low flow region, for two smaller burners, 0.546 and 0.311 centimeter in diameter. Because of unusually smooth inlet conditions, flow in the 0.546-centimeter burner did not become turbulent until a Reynolds number of about 6000 was reached. In order to obtain a larger experimental region of turbulent blowoff, the burner inlet was very loosely packed with steel wool. This procedure induced steady turbulence at a Reynolds number of about 3000. Data for both conditions are shown in figure 6. It should be noted that the blowoff curve in the turbulent region is independent of the Reynolds number at which steady turbulence is achieved. That is, above $Re = 6000$ blowoff data from the disturbed and undisturbed 0.546-centimeter burner lie in a single curve. With the smallest burner (0.311-cm diam.) the onset of steady turbulence was accompanied by the discontinuity in the blowoff curve at a Reynolds number of about 3000 that is shown as a dashed line in figure 6.

The general blowoff curve may be divided into several regions with increasing Reynolds number. (In figs. 5 and 6 a line of constant Reynolds number is represented by $\bar{P}U = \text{constant}$.) First, there is a region of partial wall quenching where $\partial \log \bar{U}_{bo} / \partial \log P$ is negative (α of fig. 5(d)). Second, there is a region of normal laminar blowoff where $\partial \log \bar{U}_{bo} / \partial \log P$ is infinite and then positive (β of fig. 5(d)). Third, there is a region of laminar-turbulent transition. This region corresponds, in terms of Reynolds number, to the transition region for flashback, but effects on the blowoff curve are not at all pronounced (γ of fig. 5(d)). Finally at a critical Reynolds number (in fig. 5 about 2500) the curve breaks sharply upward so that $\partial \log \bar{U}_{bo} / \partial \log P$ approaches zero. At some mass flow rate a velocity is reached above which a flame cannot exist for a given equivalence ratio and burner diameter. The blowoff curve may even bend backward so that $\partial \log \bar{U}_{bo} / \partial \log P$ assumes a negative value at high mass flow rates.

In the low-flow region it is possible, by extrapolation of blowoff and flashback data to a point (q of fig. 5), to estimate a quenching pressure and the pressure dependence of quenching diameter. Actual quenching pressures obtained in this way are considerably higher than

those predicted in reference 4 (perhaps because of uncertainty introduced by the long extrapolation imposed by restrictions on the apparatus). However, the quenching diameter obtained in this way is very nearly inversely proportional to pressure; this result is in agreement with reference 4.

The region of normal laminar blowoff (as distinguished from the region of partial quenching) may be taken to be bounded on the low-flow side by the point at which \bar{U}_{bo} goes through a minimum and on the high-flow side by the point at which flames assume a nearly steady turbulent appearance. For the two larger burners this coincides roughly with the point at which the curves break sharply upward. Thus, a large portion of the transition region is considered as included in the laminar region. This may be justified by the fact that the blowoff curve throughout most of the transition region is a smooth continuation of the normal laminar curve.

Effect of pressure and tube diameter. - In the past, the blowoff of laminar and turbulent burner flames has been successfully correlated as a function of burner diameter and equivalence ratio by a boundary velocity gradient g_{bo} (ref. 13). In practice, this has been calculated in exactly the same way as the boundary velocity gradient for flashback. Thus, in the laminar region

$$g_{bo} = 8\bar{U}_{bo}/D \quad (20)$$

and in the turbulent region

$$g_{bo} = 0.023 \frac{Re^{0.8} \bar{U}_{bo}}{D} \quad (21)$$

It is difficult to relate the observed correlation to a detailed mechanism because of two experimental complications. First, if conditions are close to blowoff, a flame will be stabilized at some distance above the burner rim; this distance will be a function of pressure, stream velocity, and initial mixture (ref. 1, p. 80). Therefore, the flame will be stabilized in the mixing region of the free jet so that a model based on wall friction within a pipe may not be valid. Second, the burning velocity at the base of the flame will not correspond to the burning velocity of the initial mixture because of diffusion near the base of the free jet. This will be particularly important for rich flames burning in secondary air. In general, then, if a critical boundary velocity gradient for blowoff is described as

$$g_{bo} = U_b/\delta_{bo} \quad (22)$$

both U_b and g_{bo} will be uncertain, and the degree of uncertainty will be a function of pressure, stream velocity, and initial mixture. Since, in spite of this uncertainty, a critical boundary velocity gradient has served to correlate blowoff data at constant pressure, it was of interest to examine the effect of pressure and burner diameter for a constant initial mixture. For data plotted in the form of figures 5 and 6, three conditions must be met in order that the velocity gradient model be successful. First, large portions of the laminar and turbulent blowoff curves should be described by straight lines if $\log P$ is plotted against $\log \bar{U}_{bo}$ at constant D . Second, g_{bo} and $g_{bo,t}$ should be proportional to g_f and $g_{f,t}$, respectively. This means that the pressure and diameter dependence of the critical gradients should be the same for blowoff and flashback. Third, the critical boundary velocity gradient for blowoff should be independent of burner diameter. In the turbulent region, this condition implies that the critical mean blowoff velocity should also be nearly independent of burner diameter, since an equation of the form of equation (11) should hold for blowoff.

Figures 5 and 6 show that the first condition is not met. Even if the region of partial wall quenching is not considered, the laminar blowoff curve shows considerable curvature. The turbulent portion is more nearly linear, but is not entirely free from curvature.

The second condition is not met either. Figure 7 shows a log-log plot of g_{bo} against pressure. Data are taken from the "normal laminar" portions of figures 5 and 6. Any reasonable average value for the pressure dependence of g_{bo} would be two or three times larger than the value for g_f and thus would have no meaning in terms of the simple model. With regard to the turbulent region, the proportionality of $g_{bo,t}$ and $g_{f,t}$ implies that the blowoff curve ($\log \bar{U}$ plotted against $\log P$) should break sharply upward with the onset of turbulence in a fashion similar to the behavior of the flashback curve. This is actually observed in figures 5 and 6; however, results are not sufficiently consistent to warrant quantitative discussion.

Figure 7 also shows that g_{bo} is somewhat dependent on burner diameter, particularly for smaller burners. Furthermore, in the turbulent region the critical mean blowoff velocity is rather strongly dependent on burner diameter. If observed or estimated values for this maximum over-all blowoff velocity are plotted against burner diameter, the observed value of the pressure exponent is about -0.5. This is shown in figure 8. This result indicates that increasing burner diameter will actually decrease the stability of a burner flame to blowoff. Thus, the third condition is satisfied in neither laminar nor turbulent regions.

Generally, it must be concluded that the velocity gradient model does not explain the dependence of either laminar or turbulent blowoff on pressure and burner diameter.

Recently two rather limited theoretical treatments have been offered which lead to explicit expressions for the pressure dependence of critical blowoff velocity. In one treatment (ref. 14) it is assumed that blowoff occurs because of the interruption of flame propagation caused by a high velocity gradient near the flame base. In the other treatment (ref. 15, p. 182) blowoff is assumed to occur simply because the mass flow rate through the burner exceeds a critical mass reaction rate. Both treatments concern piloted turbulent burner flames. However, since neither treatment considers any specific effects which a pilot might have on flame stability, it is of interest to see how well each of them describes the blowoff of turbulent flames stabilized without a pilot.

In reference 14 it is shown that a high boundary velocity gradient near the base of a turbulent flame could induce instability by reducing the local flame speed. A relation is derived which may be expressed as

$$\beta' \propto \bar{U}^{7/8} D^{-1/8} P^{-(1/8+n)} \quad (23)$$

The condition for the interruption of the flame propagation was that β' assume a critical value. Setting $\beta' = \text{Constant}$ and using $n = 0.23$ (ref. 3) give

$$\bar{U}_{bo} \propto P^{0.41} D^{0.125} \quad (24)$$

By reference to figures 5 and 8, it may be seen that equation (24) does not adequately describe blowoff results, particularly with regard to the dependence of blowoff velocity on burner diameter.

Reference 15 (p. 182) also derives an expression for the critical blowoff velocity of piloted turbulent burner flames. In this case the criterion for flame extinction is that the mass flow rate exceed the total mass reaction rate. This leads to an expression

$$\bar{U}_{bo} \leq D F U_b^2 \times \text{Constant} \quad (25)$$

Since most combustion systems follow an equation of the form

$$U_b = U_b^0 P^n \quad (26)$$

equation (25) may be written as

$$\bar{U}_{bo} \leq D_p^{2n+1} \times \text{Constant} \quad (27)$$

For hydrogen-air flames, this becomes

$$\bar{U}_{bo} \propto P^{1.46} D \quad (28)$$

Both pressure and diameter exponents are very much larger than those actually observed. This may be due to the exceedingly simple model of turbulent flame stabilization adopted in reference 15, which would predict much higher values of \bar{U}_{bo} than are actually observed. The inequality sign in equation (27) may serve to represent the fact that real burner flames are much more sensitive to external disturbances than the model of reference 15 would predict.

Although neither treatment can be considered satisfactory, equation (24) represents the data more closely than equation (28) with respect to both pressure and burner diameter. It appears that whatever weaknesses may be involved in the model of reference 14, a consideration of shear near the base of a turbulent flame appears to give somewhat closer agreement with experiment than a consideration of mass flow and mass reaction rates only.

SUMMARY OF RESULTS

Stability limits of laminar and turbulent hydrogen-air burner flames were measured over a range of subatmospheric pressures. The following results were obtained:

1. The pressure exponent for the critical flashback boundary velocity gradient was the same for both laminar and turbulent flames. The composition at which it peaked was also the same.
2. The turbulent-to-laminar ratio of critical flashback boundary velocity gradients was 2.8. The difference between the gradients was not caused by an increased burning velocity for the turbulent case, but rather implied that the penetration distance for turbulent flashback was about 1/3 of the penetration distance for the laminar case.
3. Turbulent blowoff velocity was nearly independent of pressure and varied approximately with the inverse square root of burner diameter. None of the current mechanisms of flame blowoff predict these results.

4. Extrapolation of stability loops to the quenching point showed that the quenching pressure was inversely proportional to burner diameter. The actual pressures obtained were higher than those obtained by other methods.

Lewis Flight Propulsion Laboratory
National Advisory Committee for Aeronautics
Cleveland, Ohio, January 29, 1957

REFERENCES

1. Wohl, Kurt: Quenching, Flash-Back, Blow-Off - Theory and Experiment. Fourth Symposium (International) on Combustion, The Williams & Wilkins Co. (Baltimore) 1953, pp. 68-89.
2. Wolfhard, H. G.: Die Eigenschaften stationäreer Flammen im Unterdruck. Zs.f. Tech. Phys., Bd 24, Nr. 9, 1943, pp. 206-211.
3. Fine, Burton: Stability Limits and Burning Velocities of Laminar Hydrogen-Air Flames at Reduced Pressure. NACA TN 3833, 1956.
4. Potter, A. E., and Berlad, A. L.: The Effect of Fuel Type and Pressure on Flame Quenching. Paper presented at Sixth Symposium (International) on Combustion, New Haven (Conn.), Aug. 19-24, 1956.
5. Von Elbe, Guenther, and Mentser, Morris: Further Studies of the Structure and Stability of Burner Flames. Jour. Chem. Phys., vol. 13, no. 2, Feb. 1945, pp. 89-100.
6. Fine, Burton D., and Wagner, Paul: Space Heating Rates for Some Premixed Turbulent Propane-Air Flames. NACA TN 3277, 1956.
7. Lewis, Bernard, and Von Elbe, Guenther: Combustion, Flames and Explosions of Gases. Academic Press, Inc., 1951.
8. Bromley, L. A., and Wilke, C. R.: Viscosity Behavior of Gases. Ind. and Eng. Chem., vol. 43, no. 7, July 1951, pp. 1641-1648.
9. Schlichting, H.: Boundary Layer Theory. McGraw-Hill Book Co., Inc., 1955.
10. Wohl, Kurt, Kapp, Numer M., and Gazley, Carl: The Stability of Open Flames. Third Symposium on Combustion and Flame and Explosion Phenomena, The Williams & Wilkins Co. (Baltimore), 1949, pp. 3-21.

4200

11. Wohl, Kurt, Kapp, Numer M., and Gazley, Carl: The Stability of Open Flames. Meteor Rep. UAC-26, Res. Dept., United Aircraft Corp., Sept. 1948. (Proj. Meteor, U.S. Navy BuOrd Contact NOrd 9845 with M.I.T.)
12. Manton, John, and Milliken, B. B.: Study of Pressure Dependence of Burning Velocity by the Spherical Vessel Method. Proc. Gas Dynamics Symposium (Aerothermochem.), Northwestern Univ., 1956, pp. 151-157.
13. Grumer, Joseph, Harris, Margaret E., and Rowe, Valerie R.: Fundamental Flashback, Blowoff, and Yellow-Tip Limits of Fuel Gas-Air Mixtures. Rep. of Invest. 5225, Dept. Interior, Bur. Mines, July 1956.
14. Karlovitz, B., Denniston, D. W., Jr., Knapschaefer, D. H., and Wells, F. E.: Studies on Turbulent Flames. A. Flame Propagation Across Velocity Gradients. B. Turbulence Measurement in Flames. Fourth Symposium (International) on Combustion. The Williams & Wilkins Co. (Baltimore), 1953, pp. 613-620.
15. Spalding, D. B.: Some Fundamentals of Combustion. Academic Press, Inc., 1955.

TABLE I. - FLASHBACK OF HYDROGEN-AIR FLAMES

Ambient pressure, P , cm Hg	Burner diameter, D , cm	Equivalence ratio, ϕ	Average flashback velocity, U_f , cm/sec	Critical boundary velocity gradient for laminar flashback, $S_{f,t}$, sec ⁻¹	Critical boundary velocity gradient for turbulent flashback, $S_{f,t}$	Reynolds number, Re	Ambient pressure, P , cm Hg	Burner diameter, D , cm	Equivalence ratio, ϕ	Average flashback velocity, U_f , cm/sec	Critical boundary velocity gradient for laminar flashback, $S_{f,t}$, sec ⁻¹	Critical boundary velocity gradient for turbulent flashback, $S_{f,t}$	Reynolds number, Re
70.7	1.016	0.50	517	---	6,330	2740	23.2	1.890	1.20	945	---	6,130	2570
50.5	1.459		397	2180	---	2150	26.6			954	---	6,950	2970
47.9			470	---	5,580	2420	28.3			1013	---	8,140	3360
48.9			530	---	4,380	2670	30.3			1080	---	9,330	3760
68.2			462	---	4,820	3400	33.4			1084	---	10,150	4160
72.0			510	---	5,760	3930	36.7			1080	---	10,870	4560
45.1	1.016	.80	722	5690	---	1830	38.7			1092	---	11,870	4960
45.0			842	6630	---	2150	42.5			1152	---	14,200	5750
47.3			857	---	10,940	2310	15.9	1.016	1.50	92	724	---	87
51.2			844	---	11,340	2430	16.7			119	936	---	118
54.3			896	---	13,240	2730	17.2			149	1171	---	152
58.6			923	---	14,840	3030	18.1			205	1612	---	220
72.2			933	---	17,880	3780	19.8			242	1900	---	285
32.8	1.459		722	---	558	2350	40.4			730	5750	---	1750
32.5			802	---	8,990	2600	39.4			911	7170	---	2140
44.7			755	---	7,380	3260	39.4			1078	---	12,840	2520
49.7			773	---	8,790	3770	41.8			1180	---	15,840	2930
53.1			813	---	10,150	4290	46.6			1192	---	17,590	3310
57.6			835	---	11,370	4790	50.1			1240	---	20,020	3700
60.1			890	---	13,190	5310	54.0			1270	---	22,190	4090
67.4			945	---	16,110	6320	58.8			1301	---	24,810	4550
28.6	1.890		680	---	4,260	2500	63.8			1389	---	28,790	5250
30.1			752	---	5,320	2900	72.6			1401	---	33,550	6040
33.2			770	---	6,000	3290	28.5	1.459		952	5220	---	2310
35.6			783	---	6,540	3580	28.8			1054	---	8,920	2590
39.3			804	---	7,430	4070	31.4			1172	---	11,580	3140
45.3			835	---	8,910	4860	36.5			1219	---	14,010	3690
51.1			857	---	10,280	5640	41.2			1205	---	15,122	4230
55.4			904	---	12,070	6440	45.0			1242	---	17,156	4770
45.3	1.016	.95	808	6360	---	2440	48.4			1278	---	19,123	5300
44.3			955	---	12,210	2820	53.9			1278	---	20,842	5870
50.8			945	---	13,365	3200	54.4			1348	---	23,112	6450
56.8			944	---	14,585	3570	22.3	1.890	1.50	980	---	4,150	2220
59.1			1000	---	16,702	3950	25.1			1119	---	7,910	2610
65.9			1000	---	18,222	4330	25.7			1147	---	9,010	3000
73.8			1080	---	22,156	5200	29.3			1159	---	10,190	3460
30.5	1.459		787	4200	---	2240	32.4			1136	---	10,680	4080
31.5			830	4550	---	2490	31.3			1175	---	11,010	4080
32.9			880	---	7,725	2770	34.6			1182	---	12,060	4520
34.8			910	---	8,582	3050	34.7			1136	---	11,260	4520
40.0			930	---	9,977	3560	39.3	1.016	1.80	986	7780	---	2130
45.0			950	---	11,391	4090	41.3			1110	---	13,250	2510
49.3			977	---	12,887	4610	44.8			1180	---	15,790	2910
52.3			1025	---	14,729	5150	48.8			1229	---	18,190	3300
56.9			1045	---	16,314	5690	53.3			1259	---	20,390	3690
61.0			1082	---	17,758	6210	60.7			1338	---	25,240	4470
24.8	1.890		755	3195	---	2140	66.7			1425	---	30,480	5230
25.1			878	---	5,883	2520	27.8	1.459		930	5110	---	2040
28.4			899	---	6,776	2890	28.5			1030	---	8,006	2320
31.3			915	---	7,561	3270	29.2			1119	---	9,480	2580
33.8			943	---	8,488	3640	37.1			1160	---	12,250	3400
37.3			943	---	9,185	4020	39.5			1250	---	14,730	3920
39.8			963	---	10,047	4380	44.9			1261	---	16,580	4470
41.6			1000	---	11,159	4760	47.9			1320	---	18,960	4990
45.3			1000	---	11,925	5150	52.5			1335	---	20,820	5540
17.3	1.016	1.10	85	869	---	92	23.7	1.89		1080	---	7,140	2610
17.8			122	960	---	136	27.1			1090	---	8,090	3010
18.8			147	1157	---	173	28.0			1055	---	7,830	3010
19.5			178	1400	---	217	28.7			1171	---	9,630	3440
10.8	1.459		65.2	358	---	63	31.6			1190	---	10,710	3850
11.4			92.5	507	---	95	33.5			1245	---	12,170	4270
12.3			114	625	---	125	36.1			1262	---	13,240	4660
12.9			128	702	---	149	45.7			786	6040	---	1800
13.6			165	904	---	202	48.2			889	7000	---	2200
14.4			196	1075	---	254	48.7			1084	---	13,020	2600
41.5	1.016	1.20	850	6700	---	2220	49.9			1176	---	15,900	3010
43.0			983	---	12,200	2660	55.5			1195	---	17,810	3410
46.9			1028	---	14,170	3040	61.6			1205	---	19,680	3810
50.7			1071	---	16,240	3420	65.9			1251	---	22,190	4240
53.7			1127	---	18,840	3820	71.7			1253	---	23,620	4610
63.4			1192	---	23,390	4770	32.0	1.459		895	4910	---	2110
69.4			1260	---	27,970	5510	33.9			1066	---	9,090	2640
29.9	1.459		785	4300	---	2120	38.7			1129	---	11,210	3220
29.9			885	4850	---	2390	43.9			1171	---	13,240	3790
30.3			975	---	8,450	2670	48.6			1213	---	15,310	4340
37.9			972	---	10,050	3330	25.1	1.89		1040	---	8,490	2490
39.7			1077	---	12,550	3870	27.1			1130	---	9,020	2920
44.2			1096	---	14,110	4390	28.6			1228	---	9,720	3360
46.7			1158	---	16,280	4900	55.0			904	---	9,390	2280
50.2			1190	---	18,110	5410	57.1			1031	---	12,240	2720
54.1			1211	---	19,650	5940	65.1			1056	---	14,200	3140
56.7			1259	---	22,100	6470	70.8			1089	---	16,080	3550

4-200

CQ-3 back

TABLE II. - FLASHBACK OF TURBULENT

HYDROGEN-AIR FLAMES

Equiva- lence ratio, ϕ	$\frac{\partial \log \xi_{f,t}}{\partial \log P}$	$\left(\frac{\xi_{f,t}}{\xi_f}\right)_p$
0.50	0.87	-----
.80	1.44	2.5 to 3.3
.95	1.22	2.5 to 2.9
1.20	1.38	-----
1.50	1.28	2.6
1.80	1.34	2.7
2.25	1.23	3.2
3.00	1.26	-----

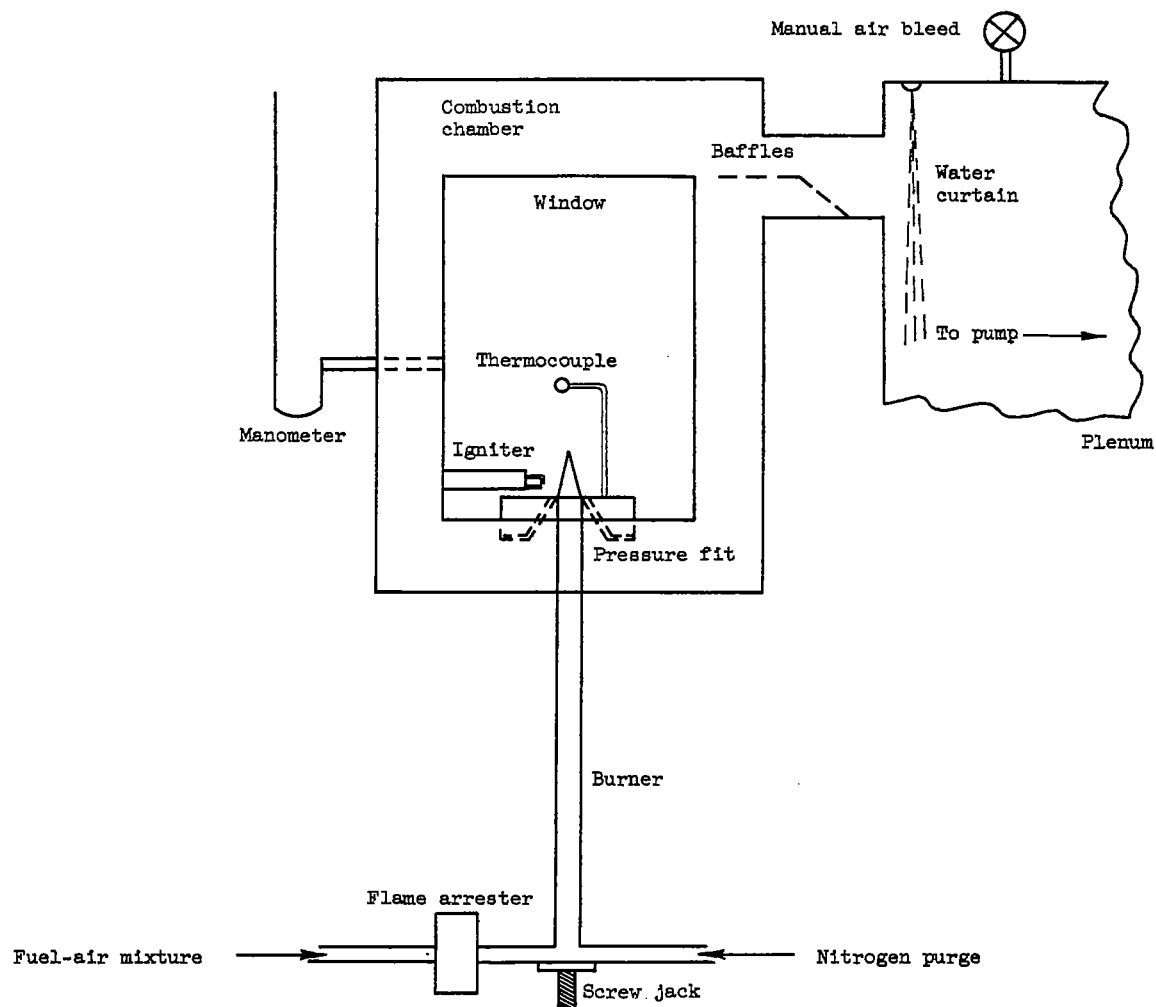


Figure 1. - Combustion apparatus.

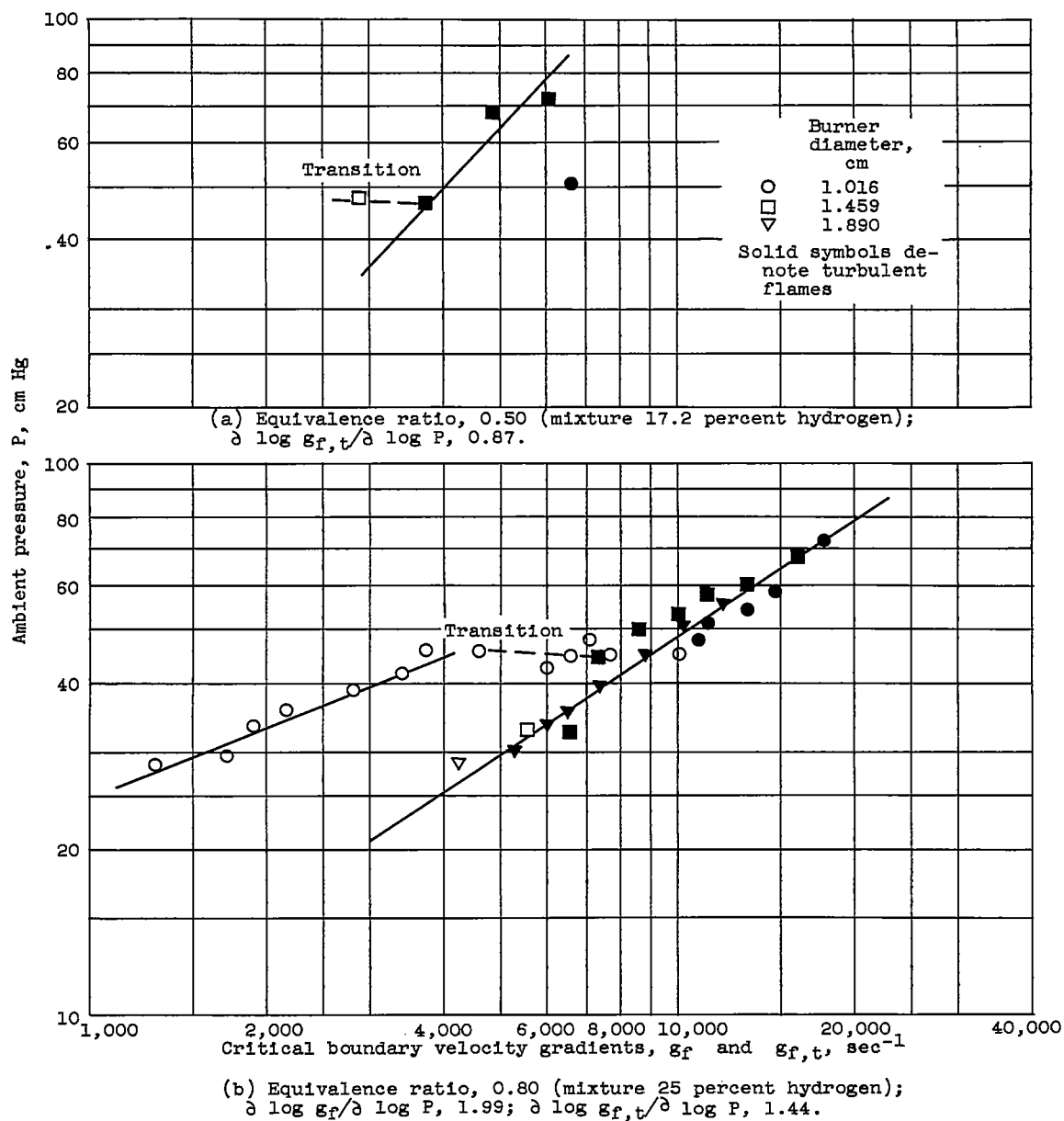


Figure 2. - Flashback of laminar and turbulent hydrogen-air flames.

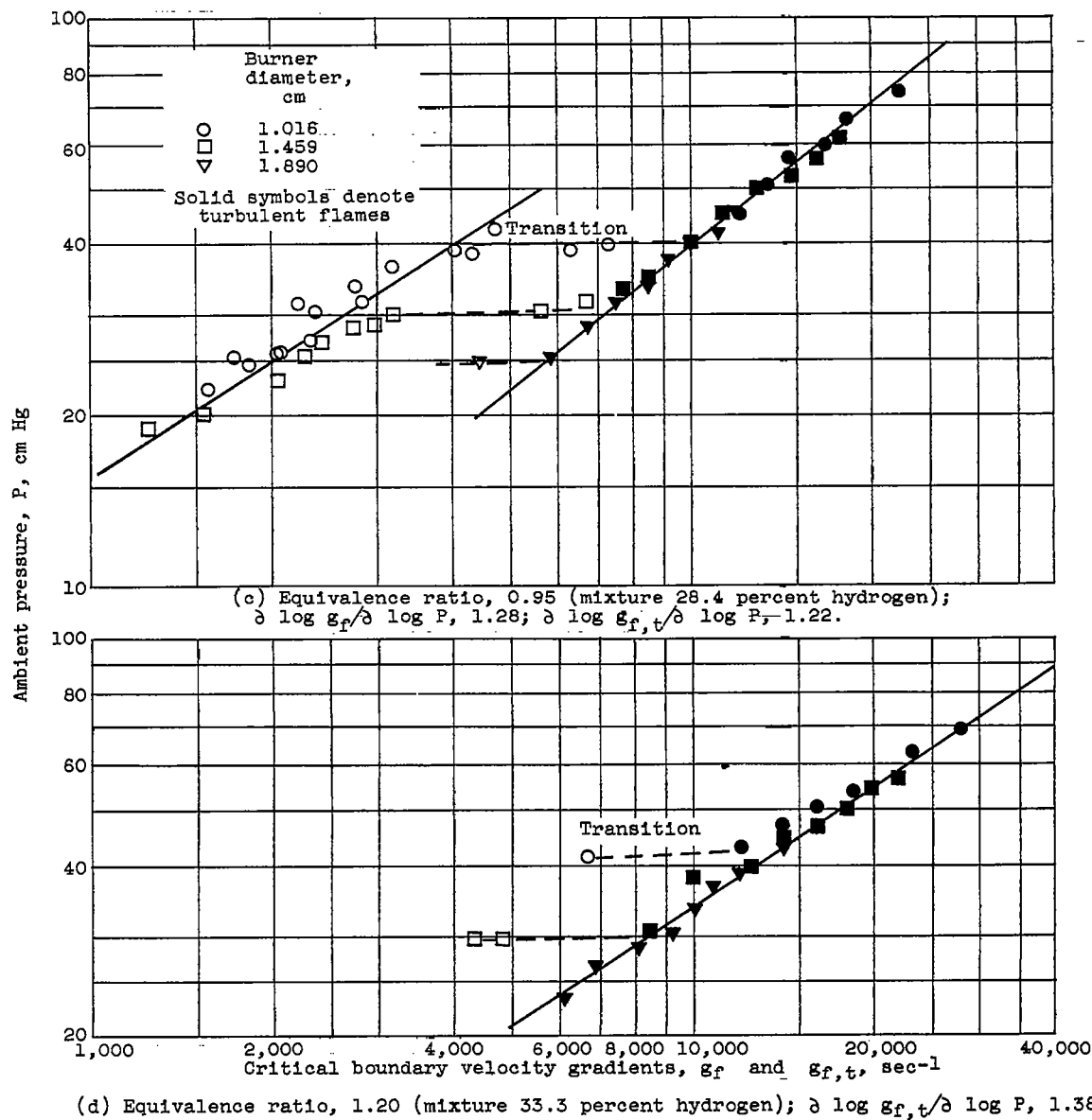


Figure 2. - Continued. Flashback of laminar and turbulent hydrogen-air flames.

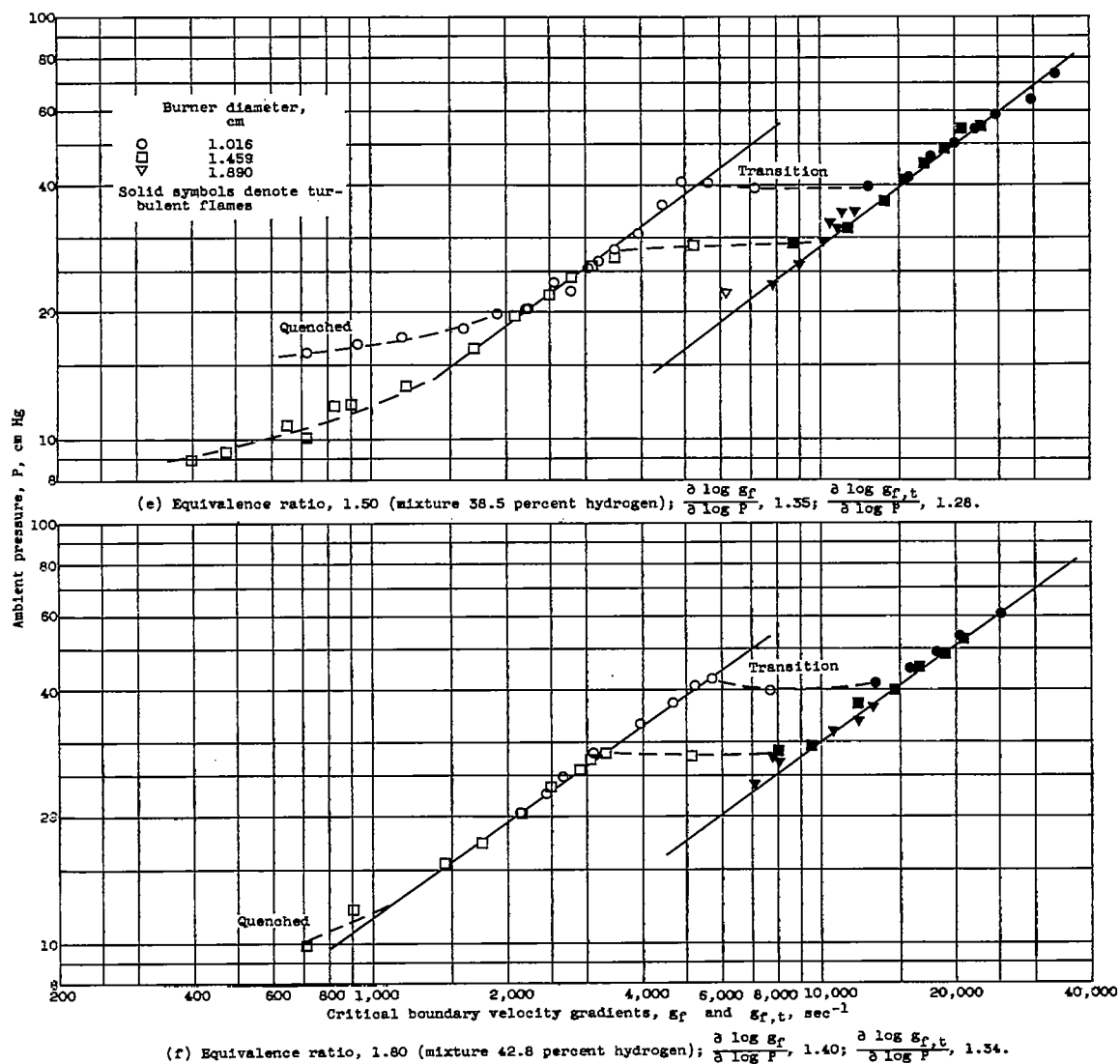


Figure 2. - Continued. Flashback of laminar and turbulent hydrogen-air flames.

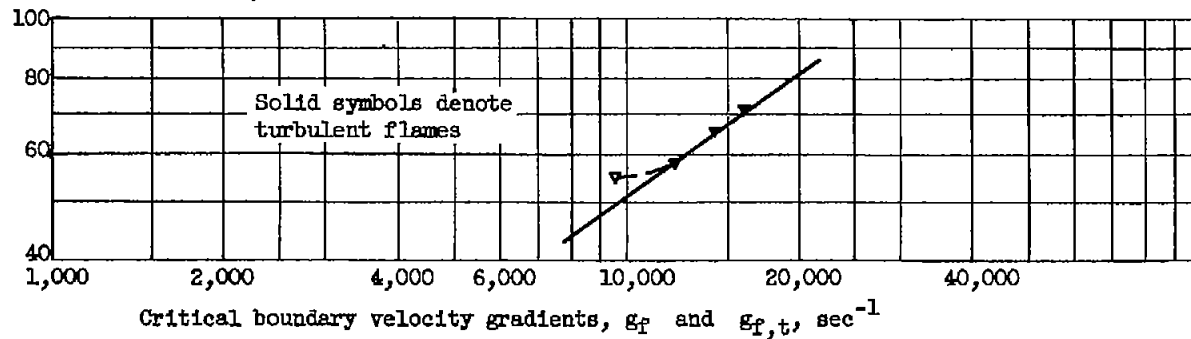
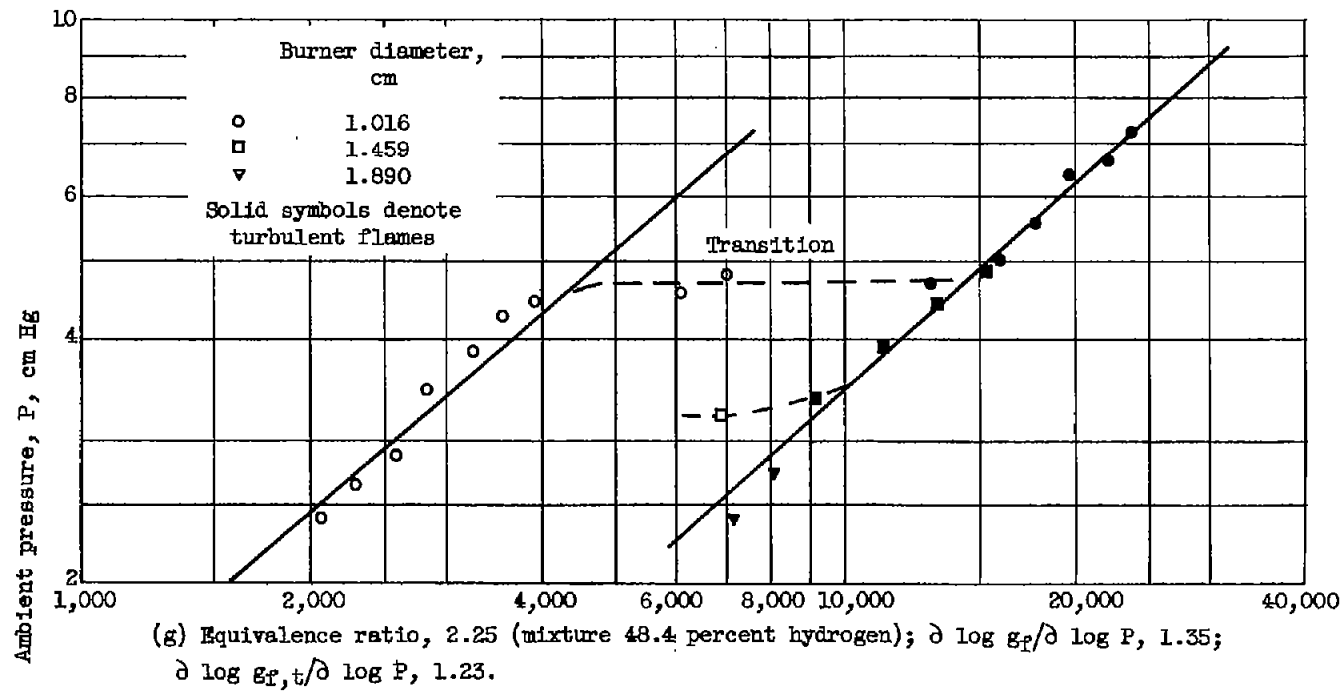


Figure 2. - Concluded. Flashback of laminar and turbulent hydrogen-air flames.

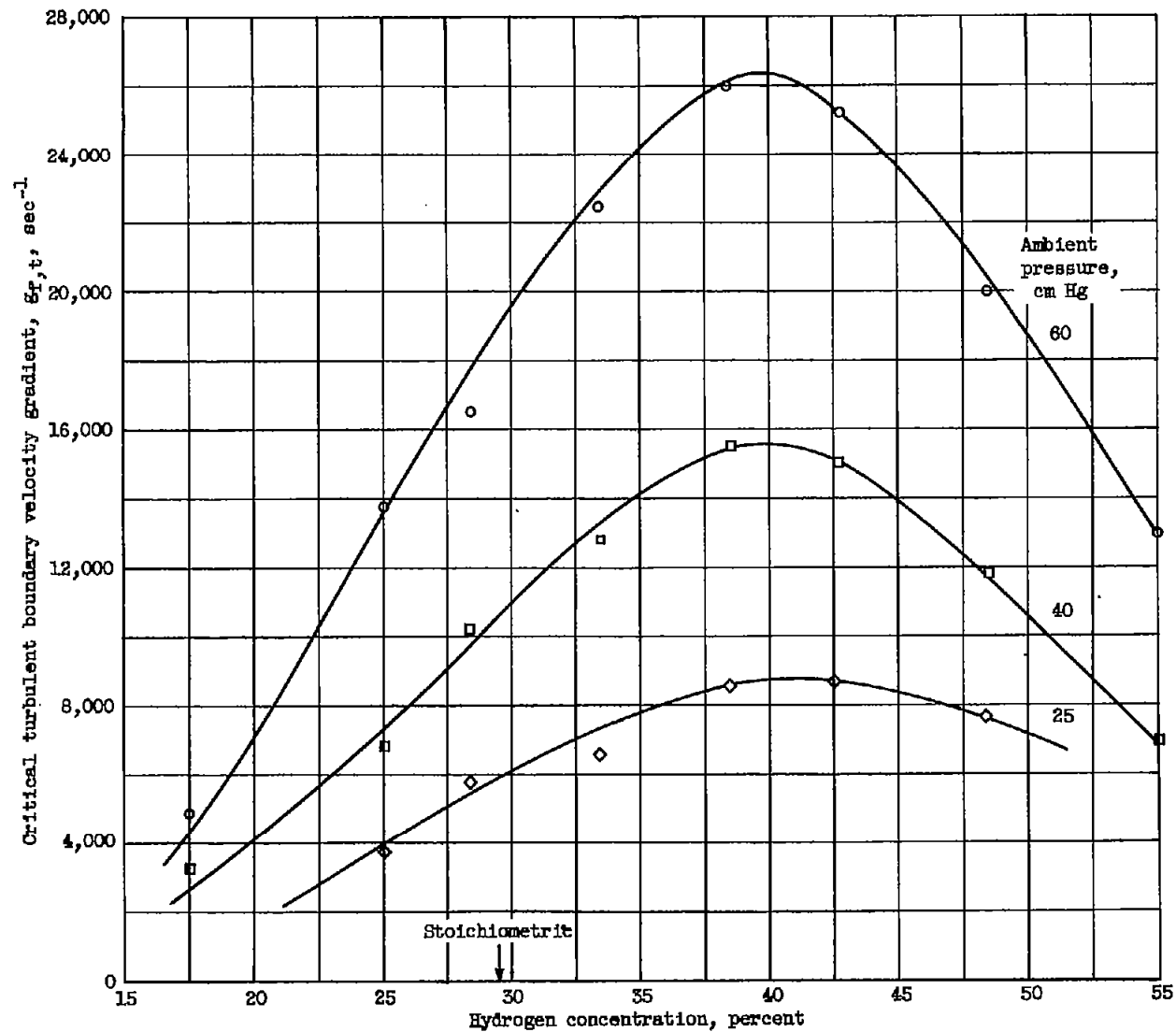


Figure 3. - Turbulent flashback velocity gradient as function of composition at constant pressure.

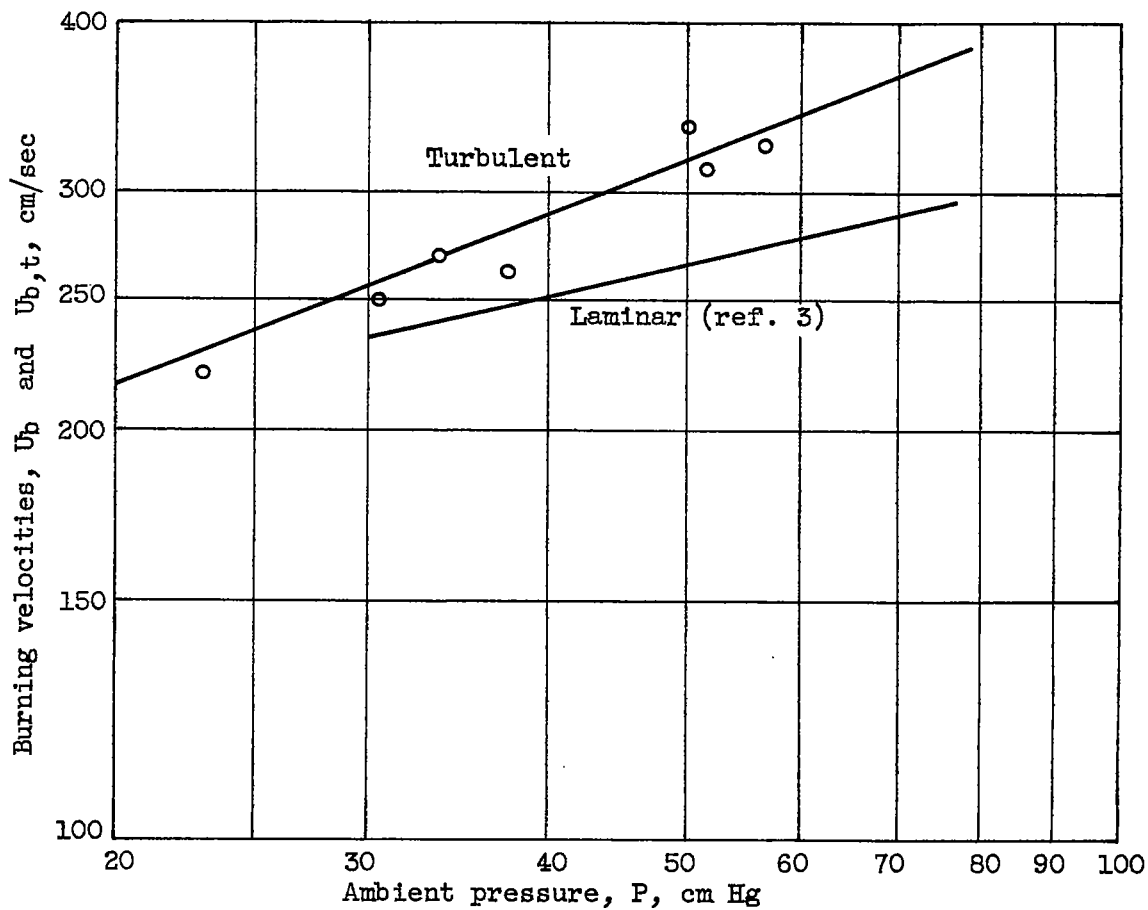
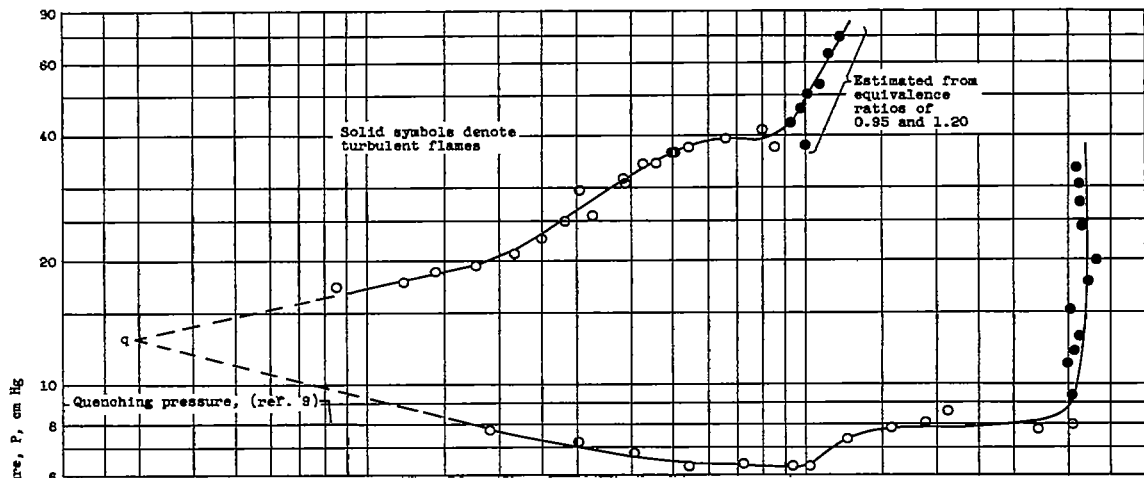
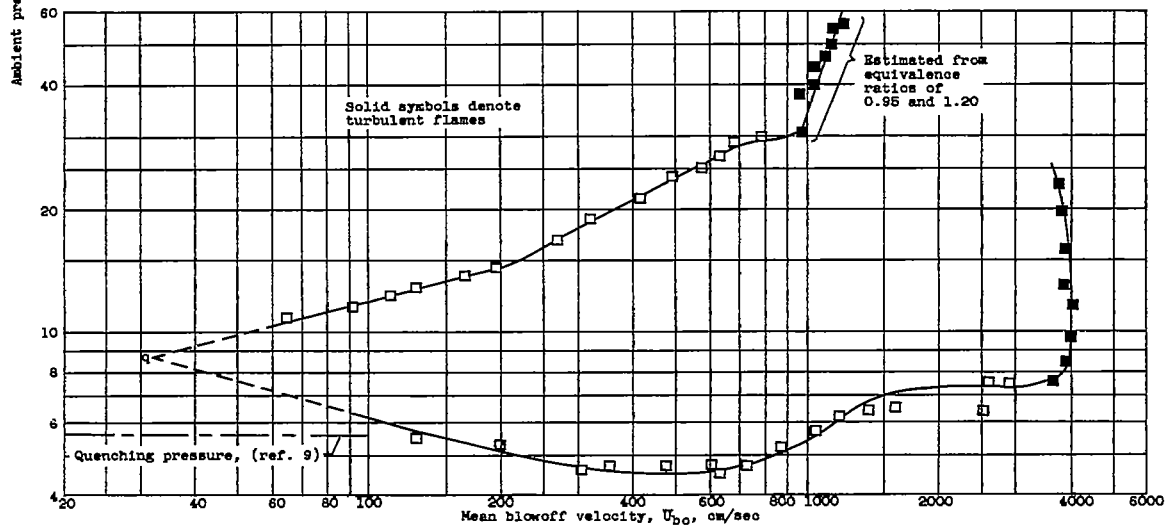


Figure 4. - Laminar and turbulent burning velocity for hydrogen-air flames as function of pressure. Equivalence ratio, 1.8.



(a) Burner diameter, 1.016 centimeters; equivalence ratio, 1.10 (mixture 31.5 percent hydrogen).



(b) Burner diameter, 1.459 centimeters; equivalence ratio, 1.10 (mixture 31.5 percent hydrogen).

Figure 5. - Stability loop for hydrogen-air flames.

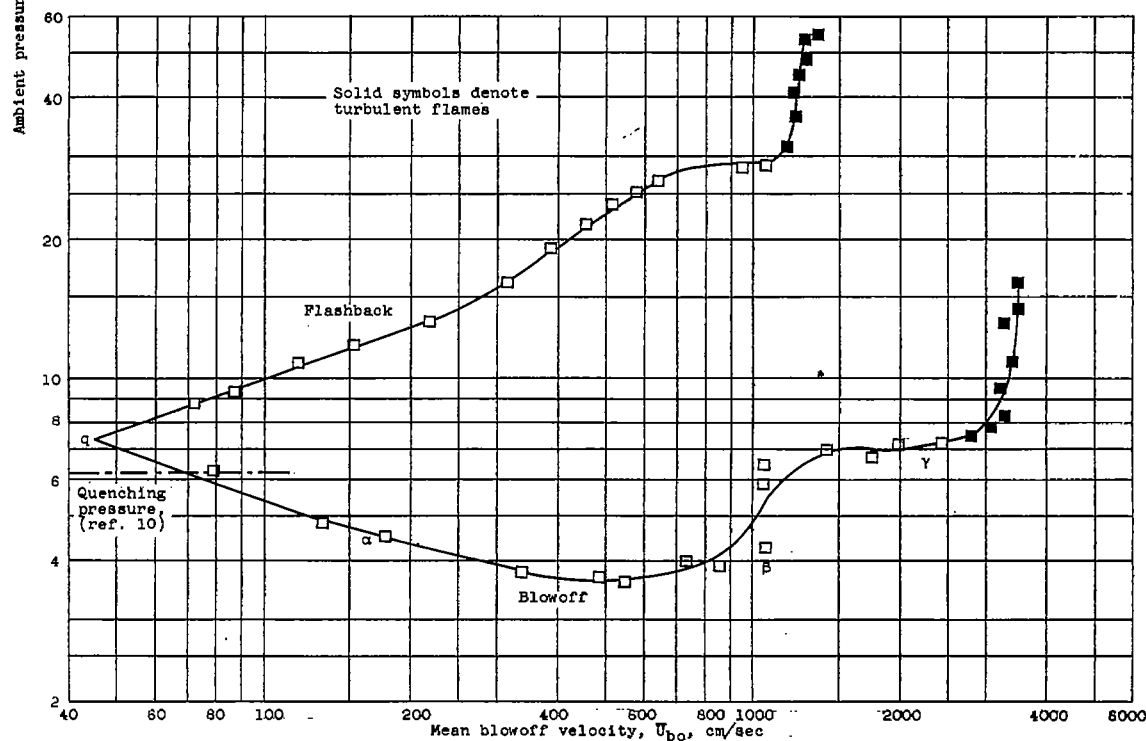
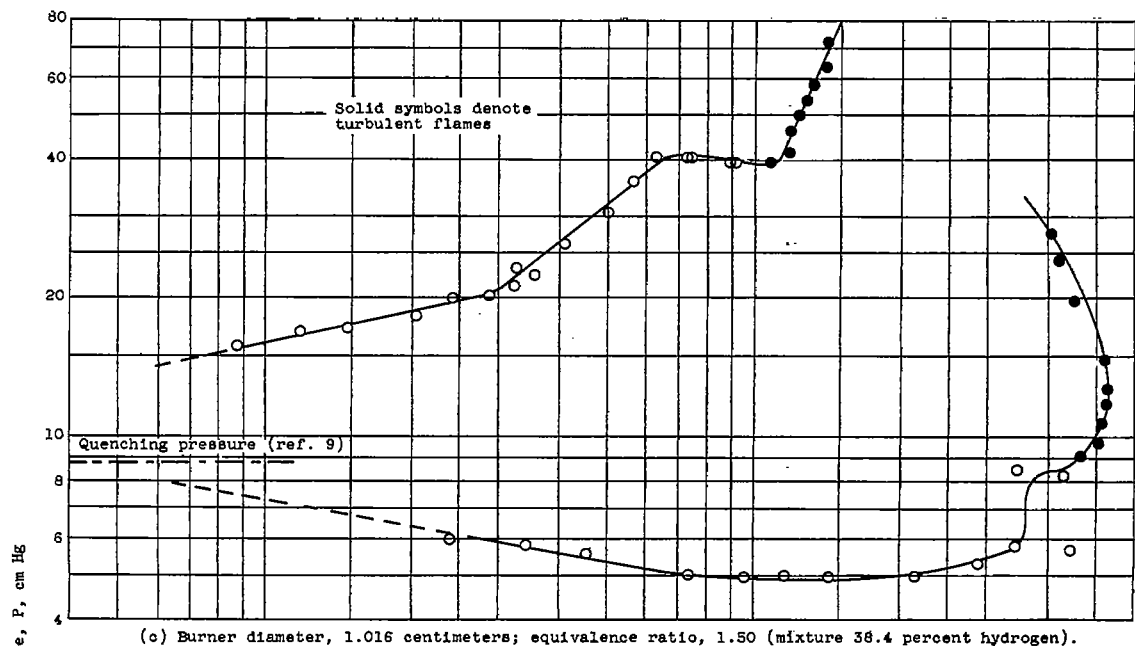
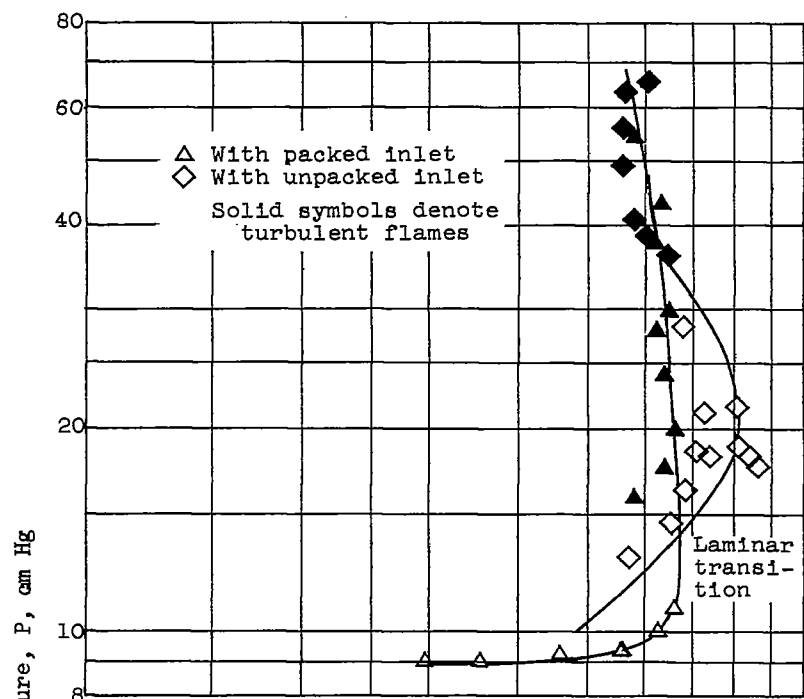
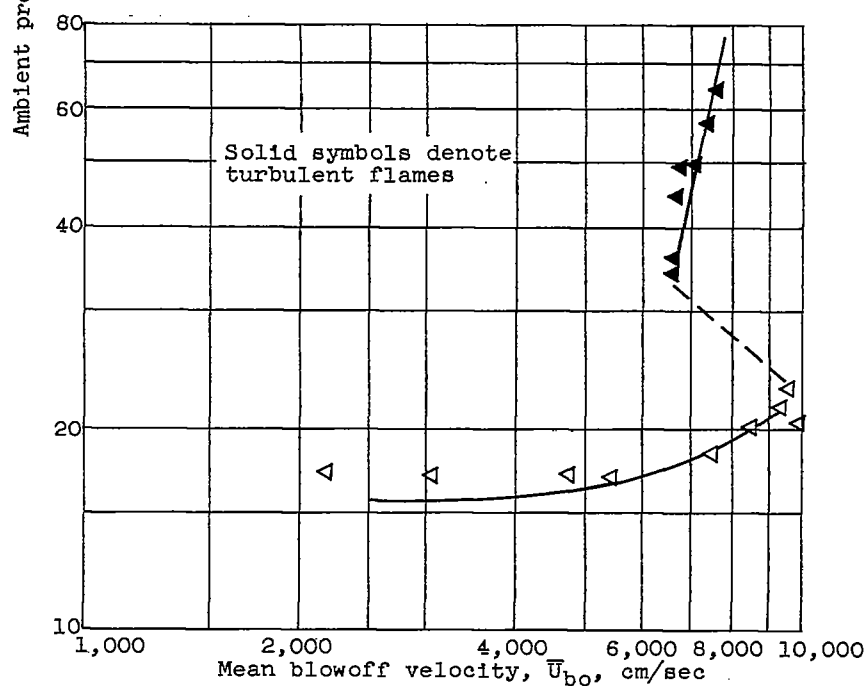


Figure 5. - Concluded. Stability loop for hydrogen-air flames.



(a) Burner diameter, 0.546 centimeter.



(b) Burner diameter, 0.311 centimeter.

Figure 6. - Blowoff of hydrogen-air flames from small burners. Equivalence ratio, 1.10.

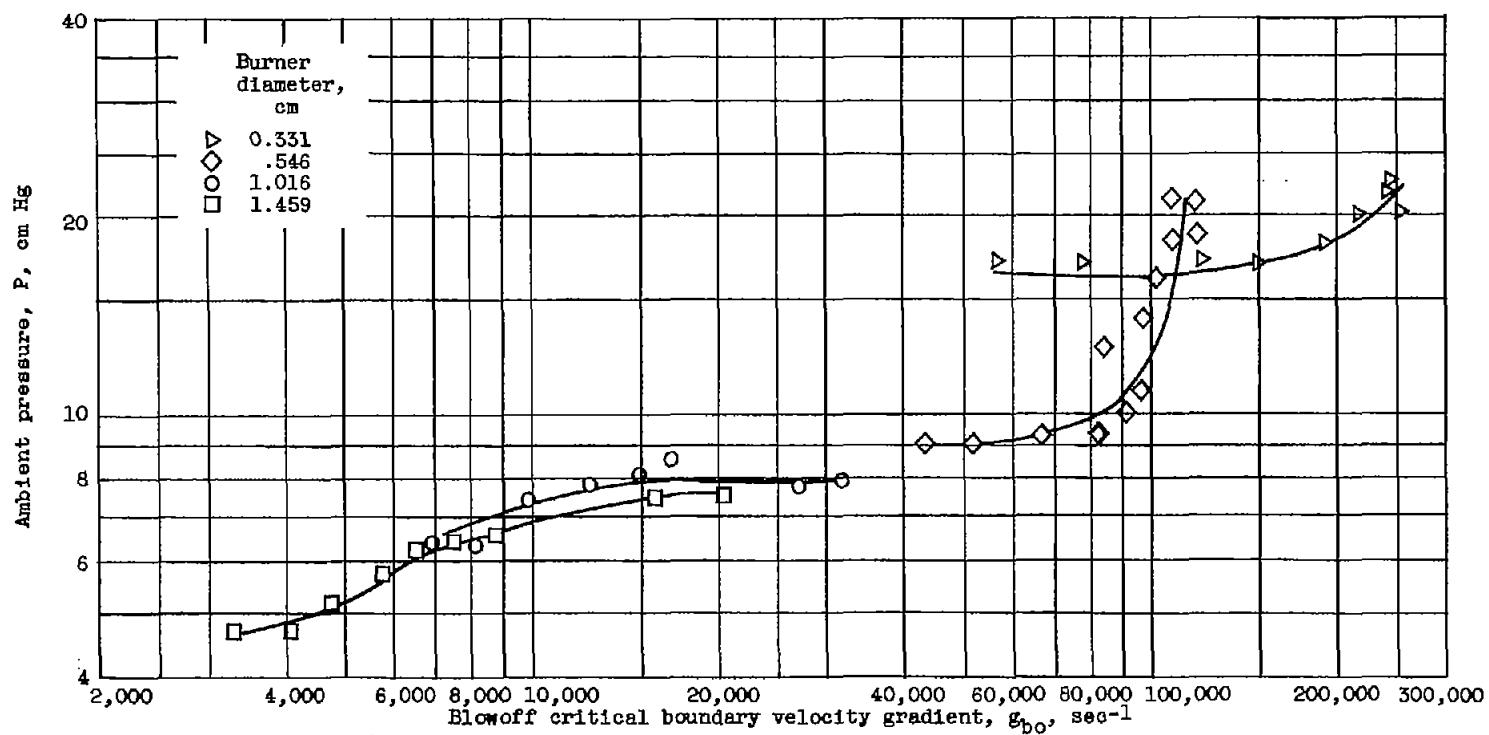


Figure 7. - Comparison of data from figures 5 and 6 for blowoff of laminar hydrogen-air flames. Equivalence ratio, 1.10.

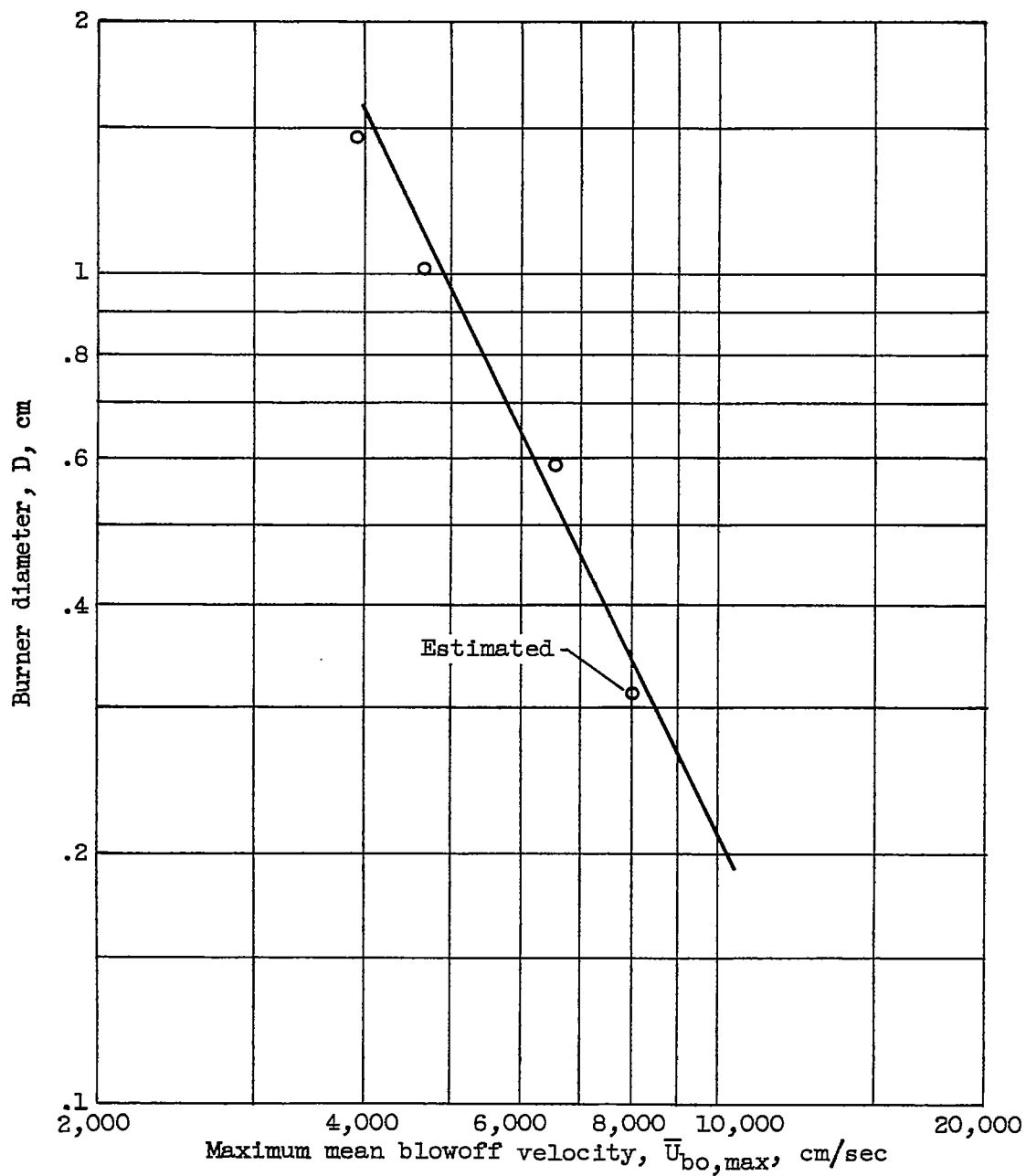


Figure 8. - Dependence of turbulent blowoff velocity on burner diameter. Equivalence ratio, 1.1; diameter exponent at blowoff, m_{bo} , -0.47.